Atmos. Chem. Phys., 18, 5359–5370, 2018
https://doi.org/10.5194/acp-18-5359-2018

Atmospheric Chemistry and Physics
Open Access
EGU

Using the Fire Weather Index (FWI) to improve the estimation of fire emissions from fire radiative power (FRP) observations

Francesca Di Giuseppe[1], **Samuel Rémy**[2], **Florian Pappenberger**[1], **and Fredrik Wetterhall**[1]

[1]European Centre for Medium-Range Weather Forecasts (ECMWF), Reading, UK
[2]Institut Pierre-Simon Laplace (IPSL), CNRS/UPMC, Paris, France

Correspondence: Francesca Di Giuseppe (f.digiuseppe@ecmwf.int)

Received: 23 August 2017 – Discussion started: 26 September 2017
Revised: 1 February 2018 – Accepted: 28 February 2018 – Published: 20 April 2018

Abstract. The atmospheric composition analysis and forecast for the European Copernicus Atmosphere Monitoring Services (CAMS) relies on biomass-burning fire emission estimates from the Global Fire Assimilation System (GFAS). The GFAS is a global system and converts fire radiative power (FRP) observations from MODIS satellites into smoke constituents. Missing observations are filled in using persistence, whereby observed FRP values from the previous day are progressed in time until a new observation is recorded. One of the consequences of this assumption is an increase of fire duration, which in turn translates into an increase of emissions estimated from fires compared to what is available from observations. In this study persistence is replaced by modelled predictions using the Canadian Fire Weather Index (FWI), which describes how atmospheric conditions affect the vegetation moisture content and ultimately fire duration. The skill in predicting emissions from biomass burning is improved with the new technique, which indicates that using an FWI-based model to infer emissions from FRP is better than persistence when observations are not available.

1 Introduction

Emissions generated from biomass burning contribute extensively to the global budget of several atmospheric constituents such as aerosols, carbon monoxide (CO) and carbon dioxide (CO_2). The annual emission of several gases generated during combustion is comparable to what is emitted from anthropogenic sources (Crutzen et al., 1979). Chemical fluxes from fires need to be accounted for in global systems that monitor and forecast atmospheric composition, such as the European Copernicus Atmosphere Monitoring Services (CAMS). Since 2012, the Global Fire Assimilation System (GFAS)[1] has provided global fire emissions to the atmospheric composition model operated by CAMS: the Integrated Forecasting System (IFS). GFAS uses a liner relationship to convert fire radiative power (FRP) observations from the MODIS instruments (Kaufman et al., 2003) into fuel consumption. Emissions are then derived using land-use-dependent conversion factors. The current system does not explicitly forecast fire evolution.

The main shortcoming of the MODIS FRP product is the limited sampling frequency: between one and four observations per day and per satellite for each GFAS grid point (Kaiser et al., 2012). The typical coverage has a return period between 4 and 12 h for any location but this time window is often expanded by the presence of clouds, snow and ice on the ground, which interfere with the instrument detection systems (Kaufman et al., 2003). When a missing observation occurs the day after a fire has been detected, the GFAS relies on persistence. This means that values of FRP for the previous day as provided by the GFAS are progressed in time until a valid observation is detected. The assumption of persistence can potentially cause an overestimation of fire duration, and this will be more pronounced in areas of the planet that are frequently covered in clouds or where the time variability of fires is the greatest. To put things into context, the June–August 2013 observed global average fire duration calculated using MODIS observations was 4.2 days.

[1]The Global Fire Assimilation System (GFAS) was developed initially under two EU-founded projects, MACC and MACC-II. Since 2015, it has operated as part of the European Copernicus Atmosphere Monitoring Services (CAMS).

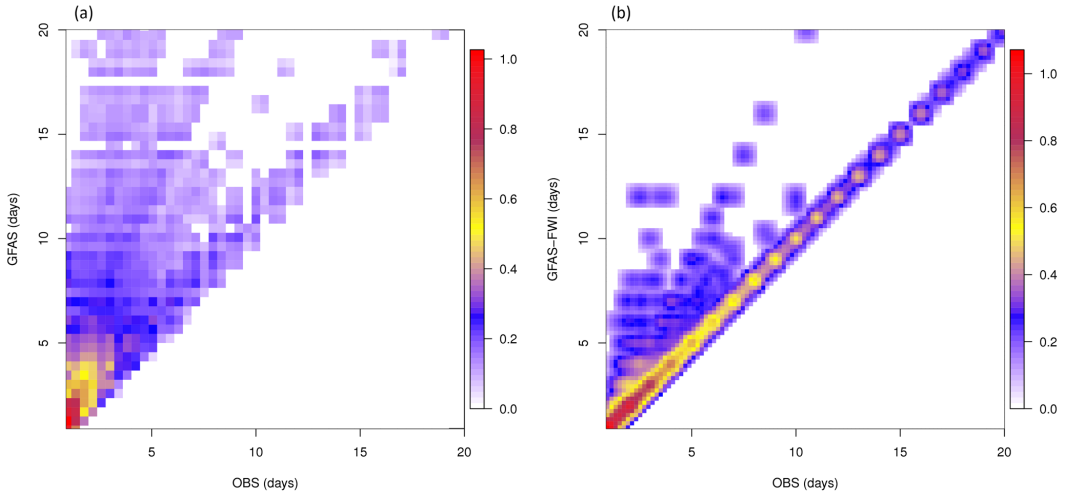

Figure 1. (a) Normalized density plot of average consecutive days of continuous fire observations as recorded by MODIS on board Aqua and Terra satellites versus the estimated values from the GFAS. The longer fire duration in the GFAS is due to the persistence assumption, which extends observations during observation blackout periods. **(b)** As before but for the application of the new FWI-based model.

By assuming persistence, the GFAS extends this duration by 1.2 days (see Fig. 1 in Sect. 3).

Increasing the temporal frequency of observations could reduce the need to resort to the persistence assumption. In 2008, the EUMETSAT Land Satellite Application Facility started the real-time production of a newly developed FRP product generated from SEVIRI observations. This product maintains SEVIRI's return (sampling) period of 15 min, which makes it capable of resolving the diurnal cycle of open fires in Africa and southern Europe with unprecedented accuracy. SEVIRI has lower spatial resolution than MODIS; the observing pixel size at nadir is 3000 m against the 1000 m of MODIS for the channels that are used in the FRP calculations. This broad spatial resolution makes small fire mappings challenging with the exclusive use of SEVIRI. Nevertheless, the high sampling frequency means fire observations can occur during brief cloud-free spells in otherwise mostly cloudy regions. In addition it covers higher latitudes than the MODIS fire products since snow and ice pixels are being processed. Despite these advantages the FRP product from SEVIRI does not provide global coverage since it only covers a geographical disc comprising Europe and Africa. Moreover, the SEVIRI FRP level 2 products undergo a different calibration procedure from that of MODIS, and the merging of the two datasets has proven to be a challenge (Roberts et al., 2011).

Given the difficulties in the use of multiple platform observations, in this paper we propose a new approach to improve the emission estimations from FRP observations based on the idea that weather plays a major role in the ignition, spread and termination of wild fires wherever there is available combustible vegetation and suitable terrain topography (Flannigan et al., 2005, 2009). The use of a fire danger index based on atmospheric parameters, such as the Fire Weather Index (FWI) (Van Wagner, 1985), is potentially a better approach to simulate the evolution of fires compared to the persistence assumption (De Groot et al., 2007). The FWI is already widely employed in fire management and control (Lee et al., 2002). However, it does not explicitly model fire evolution, but it is a measure of fire danger (Van Wagner, 1987). Even for extreme FWI values there is a need for a stochastic component, i.e. ignition, to start a fire. For this reason, situations in which FWI is high but no fire is recorded are not uncommon. Di Giuseppe et al. (2016) showed how this index can be a very good predictor of fire activity where fire is limited by moisture (e.g. boreal forests), whereas where fires are fuel-limited (e.g. in the savanna ecosystem) the stochastic component becomes dominant. In these regions using the FWI as a fire modulator could be less accurate. Still, in the proposed application FWI is used when a fire has already been detected by a valid value of FRP; therefore the random component (a.k.a. ignition) is intrinsically removed. In this situation we claim that changes in FWI can be used to predict how atmospheric temperature, humidity, precipitation and wind affect the fuel moisture content and its inflammability and therefore fire evolution (Van Wagner, 1985, 1987; Stocks et al., 1989).

The new model based on the FWI has been implemented in GFAS to account for missing observations in the MODIS FRP. Improvements in the prediction of biomass-burning emissions have been assessed for a collection of 5-day forecasts initialized on a daily basis during 3 months spanning June–August 2013.

2 Method

Fire radiative power is the radiant heat power emitted by fires and it can be related to the energy released during the combustion process, whereby carbon-based fuel is oxidized to CO_2 (Wooster et al., 2005). Measurements of FRP are proportional to the total biomass combustion and thus to emissions (van der Werf et al., 2006; Kaiser et al., 2012).

The FRP (ρ) observations from MODIS used in this study are available at 1 km resolution from the MOD14 product of MODIS Collection 6. This dataset also provides a pixel classification attribute to flag missing observations (mostly because of cloud cover) and low confidence measurements, which are disregarded by the GFAS. Valid observations are first area-weighted by the portion of satellite footprint included in the grid box area in order to provide mean FRP density on a grid box of 0.1°. They are then converted into dry matter burnt $\overline{\rho}$ following Wooster et al. (2005) and finally into emissions for 44 constituents, $\mathcal{E}_i$, using the simple formulation

$$\mathcal{E}_i = \overline{\rho} \cdot \mathcal{X}_i, \tag{1}$$

where $\mathcal{X}_i$ are conversion coefficients from Heil et al. (2010).

Since observations contain gaps due to missing data, a simple model is applied to obtain a practical estimate of current observations from earlier measurements (Kalnay, 2003). At a specific time step t the estimate for ρ_t, $\widetilde{\rho_t}$, given observation at $t-1$, is then expressed as

$$\widetilde{\rho_t} = \mathcal{O}_{t-1\to t} \cdot \rho_{t-1} + \delta\rho, \tag{2}$$

where $\delta\rho$ is the observed FRP increment in the δt time interval.

$$\delta\rho = \rho_t - \rho_{t-1} \tag{3}$$

and $\mathcal{O}$ is an "observation operator" that transfers the information at time $t-1$ to time t. As already explained, persistence is assumed in the operational version of the GFAS and the observation operator is equal to the identity operator, $\mathcal{O} \equiv \mathcal{I}$ (Kaiser et al., 2012). Therefore, in the case of a non-valid observation at time t, $\delta\rho$ becomes undefined and Eq. (2) simply reduces to $\widetilde{\rho_t} = \rho_{t-1}$. When a valid observation is available, Eq. (2) leads to $\widetilde{\rho_t} = \rho_t$.

We propose the use of a new formulation for the observation operator $\mathcal{O}$ which relies on the actual weather conditions and the fire conditions recorded the previous day (French et al., 2004). The FWI provides the base for $\mathcal{O}$. FWI is defined as the intensity of the propagating flame front depending on the quantity of energy released from a linear unit of the front itself. It is an index composed of six sub-indices referring respectively to the daily variation of water content for fuels with different response times to changes in weather conditions, the initial rate of spread for propagation, the quantity of fuel and the expected intensity of the flame front. More details on the FWI model are provided in Appendix , while full details can be found in Van Wagner (1985).

To take into account uncertainties in the weather parameters, every day an ensemble of FWI values is diagnosed from the 51 weather forecast realizations of the European Centre for Medium-Range Weather Forecasts (ECMWF) ensemble forecasting system (Buizza et al., 1999) and the ensemble mean is evaluated. Different ranges of values can correspond to different fire danger conditions in different regions. A local calibration is performed to convert the absolute value of FWI into a normalized index. This is achieved by employing historical values of FWI calculated using ECMWF reanalysis, ERA-Interim, as forcing for the period 1980–2014 (see Di Giuseppe et al., 2016 for details) and by calculating the FWI cumulative distribution function (CDF) and its inverse for each location. The observation operator $\mathcal{O}_{t-1\to t}$ is then defined as

$$\mathcal{O}_{t-1\to t} = \mathrm{CDF}^{-1}(\mathrm{FWI}(t-1)). \tag{4}$$

$\mathcal{O}$ is therefore a direct function of temperature, relative humidity, precipitation and wind through the FWI formulation. For any value of FWI at time $t-1$, $\mathcal{O}$ provides a normalized index with values in the range [0; 1], which is then multiplied by the previous day observed FRP measurements ρ_{t-1}, to provide the best FRP estimation, $\widetilde{\rho_t}$, from which biomass-burning emissions are then calculated from Eq. (1).

3 Results

To test the impact of the new observation operator on the GFAS fire emissions and on the biomass-burning aerosol plumes predicted by the Integrated Forecasting System (IFS) operated by CAMS, 3 months of simulations were performed for summer 2013. In total 90 days of new fire emission data were produced and used in the IFS (Flemming et al., 2015). For each of the 90 starting dates the IFS produced a 5-day forecast of a number of atmospheric constituents. In this paper, we focus on the impact of the new fire emissions on biomass-burning aerosols.

3.1 Consequences of the persistence assumption

Figure 1a demonstrates the more obvious consequence of the persistence assumption – the increase in mean fire duration. It shows the difference in fire duration between MODIS and the GFAS. The density plot takes into account all fires detected by MODIS instruments on board the Terra and Aqua platforms during the verification period in summer 2013. Fire duration for MODIS is defined by the number of continuous days for which FRP is available and larger than zero. Fire duration in the GFAS extends also during observation blackout periods until a valid observation confirms the end of the event. The observed global average fire duration in the MODIS dataset is 4.2 days, and by assuming persistence the

GFAS increases the fire duration by 1.2 days. In the new formulation $\mathcal{O}$ takes on values in the interval [0; 1], and FRP predicted by the new model is therefore, by construction, expected to be smaller than or equal to what is predicted by persistence. This new formulation means an overall decrease of the mean fire duration (Fig. 1b). With the new method the mean daily duration of fires is still larger with the GFAS than with MODIS, but the overestimation is reduced to 0.3 day^{-1} on average.

As the assumption of persistence produces a systematic increase in fire duration, the emissions from biomass burning are also likely to be overestimated. It is worth stressing that the reference in terms of FRP is what is recorded *only* during valid MODIS measurements, and might not be accurate. Unfortunately, the latter assumption is difficult to verify as only limited information is available on the real amount of mass fluxes released into the atmosphere during fires. Ground truth measurements for fire emissions are only available from controlled ignition experiments aiming at studying the combustion process in detail (e.g. the TROFEE campaign described in Karl et al., 2007 and Yokelson et al., 2008). These experiments are conducted at isolated spots and are not available at the global scale needed to validate the emissions calculated by the GFAS. Global coverage of biomass-burning products can be provided by sensors on board polar orbiting or geostationary satellites. However all sources of emission, including for example anthropocentric fuel burning and chemical reactions, contribute to these measurements, not only biomass combustion. Disentangling the sole contribution from fire emissions remains a challenge. Still, a strong hint that the persistence assumption is responsible for an excess overestimate of emission is provided by Fig. 2 in which the averaged carbon monoxide (CO) concentration at the surface observed by the MOPITT[2] instrument on board the Terra satellite (Deeter et al., 2003) is compared with analysis by the IFS operated by CAMS. While the most relevant source of CO is natural in origin due to photochemical reactions in the troposphere, a large contribution also arises from combustion processes, including volcanoes and fires (Kasischke and Bruhwiler, 2002). CO can therefore to some extent be used as a marker for fire activities. Comparing CO concentration for all locations for which no fire events were recorded by MODIS (i.e. FRP = 0, Fig. 2a) with locations where fire activity was detected (Fig. 2b), the increase in CO surface concentration during fire combustion is evident. This increase is correctly picked up by the CAMS analysis, which is initialized with an extra source of CO provided by the GFAS emissions. The important aspect of Fig. 2 is that when the CO source from fire emission is included the CO surface concentration is overestimated by the CAMS analysis. The mean bias (CAMS minus MOPITT) is slightly negative (−5 ppbv) when fire is not observed and becomes highly positive (+95 ppbv) in the case of fire events. Although transport and sinks could also play a role in this large overestimation, CO emissions from the GFAS are probably also overestimated.

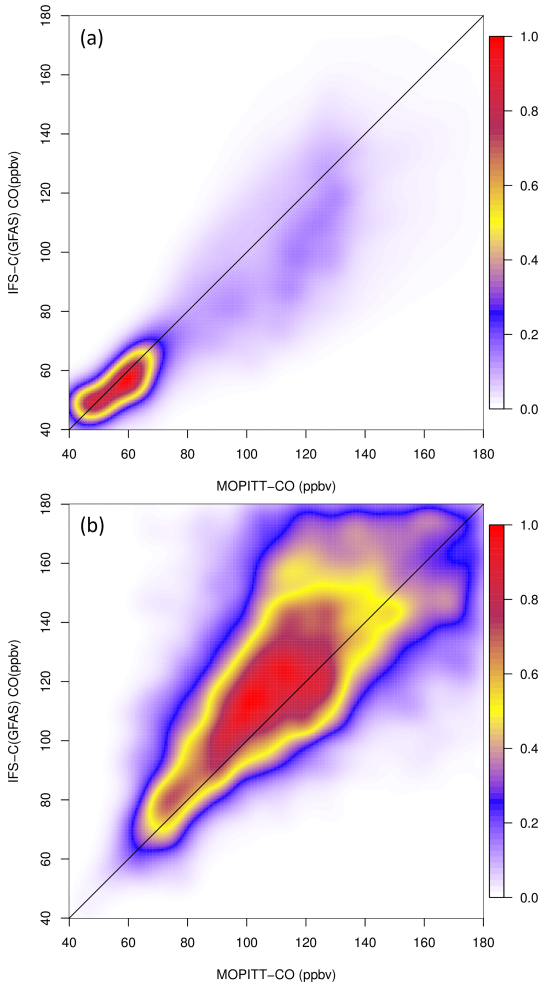

Figure 2. Normalized density plot of monthly mean surface concentration for 2013 from the MOPITT instrument on board the Terra satellite plotted against CO surface concentration analysed by CAMS. Points are grouped in locations for which fires were not detected by MODIS **(a)** and locations where fire activity was observed during that month **(b)**.

3.2 Model behaviour

To understand the impact of the new operator on the emissions we concentrate on the prediction of two fire events with different characteristics. In July 2013 large fires were recorded around the Hudson Bay in the province of Québec, Canada. Hundreds of fires consumed a total area of 616 000 ha during the first 2 weeks of July 2013. Two major events occurred, the first between 2 and 6 July with peak activity on 4 July (Fig. 3), and the second between 8 and

[2]Data used in the analysis are Version 6 Level 3 TIR/NIR products combining daytime and night-time observations. Details of the retrieval algorithm can be found in Deeter et al. (2014). Data are available at https://eosweb.larc.nasa.gov/project/mopitt.

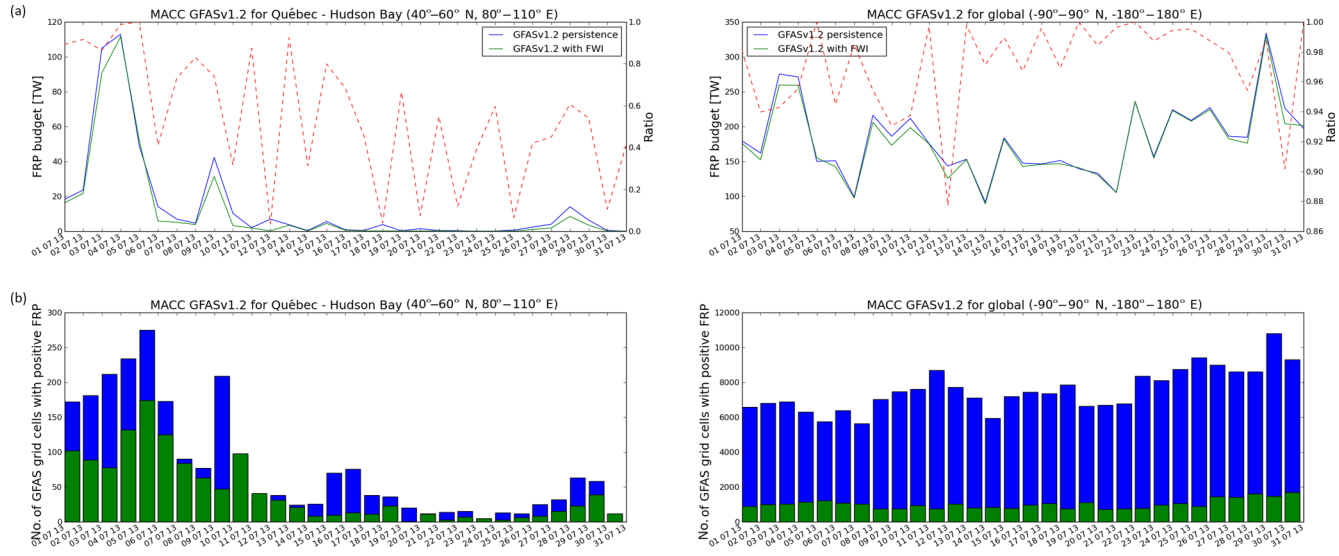

Figure 3. Budget of FRP over the Hudson Bay area and globally **(a)**. The GFAS using persistence as an observation operator is shown in blue and using FWI as an observation operator in green. The ratio between the two methods is indicated by the dashed red line. The histogram **(b)** shows the number of GFAS grid cells with positive observations for every day in July over the selected areas (blue bars) and among these the number of grid cells for which observational data were not available and FRP was estimated using either the persistence or the FWI-based model (green bar).

10 July. The smoke plumes produced by the fires in Canada reached Europe on 12 July 2013.

Figure 3 show a comparison of FRP budgets over the Hudson Bay area (40–60° N, 70–100° W) provided by the GFAS using the persistence hypothesis and FWI respectively. Using FWI reduced the total FRP by up to 80 % within the Hudson Bay area. The histogram also highlights the number of grid cells for which a positive FRP was estimated and the number of grid cells for which observational data were not available; i.e. the output of the GFAS was computed using persistence or FWI. It is interesting to note that the proportion of the GFAS grid cells without observational data increases as the fire event progresses in time, on 5–7 July. On a global scale, in around 20 % of cases, FRP from the GFAS is estimated either assuming persistence or using the FWI model.

The global budget shows a reduction of FRP computed using FWI in the range of 0 to 5 % generally, and up to nearly 10 % at times (mean ratio is 0.54 and standard deviation 0.3). The difference varies markedly from region to region; for example the FRP budget over Africa north of the equator is not affected at all by this modification (not shown). This is explained by the fact that the weather over this area is mostly dry during the summer, which means that $\mathcal{O}$ is very close to 1 and it is therefore equal to assuming persistence.

The reduction in FRP using the new operator in the GFAS had a significant impact on the simulations of biomass-burning aerosols by the IFS. It led to a maximum difference of 0.6 in the aerosol optical depth (AOD) between the two formulations (Fig. 4d). However, changes in AOD that remained confined near the fires were negligible over Europe, despite the fact that the smoke plume from Québec reached Europe on 12 July. Finally it is remarkable that changes in the biomass-burning emissions from the GFAS, which are used to initialize IFS, have an impact over the whole 5 days of model integration, signifying that these changes are compatible with the model dynamical state. On the contrary random noise would be just dumped as spurious oscillations in the model by the digital filter implemented in the IFS.

3.3 Comparison with observations

The reduction in the GFAS emissions when the new FWI model is used is consistent with the fact that large FWI decrements are more likely than increments during fire burning events. Negative increments decrease modelled FRP values, when compared to persistence, and lower the predicted emissions. It is more challenging to verify if the reductions are also improving the GFAS errors given the shortage of available measurements of fire emissions. When MODIS FRP observations are available (e.g. cloud-free pixels) it is possible to assess the predictive skill of persistence and of the model based on the FWI by using the FRP themselves as observations. Admittedly in this comparison only FRP in clear sky conditions are used even if persistence and the FWI model are instead applied to cloudy conditions i.e. when FRP is not available. However cloud coverage only affects the capability of the satellite sensors to detect FRP. It is not accounted for in the FWI equation nor is it a component of the persistence. Therefore we assume it to be acceptable to extend the verification results to all sky conditions. Figure 5 shows

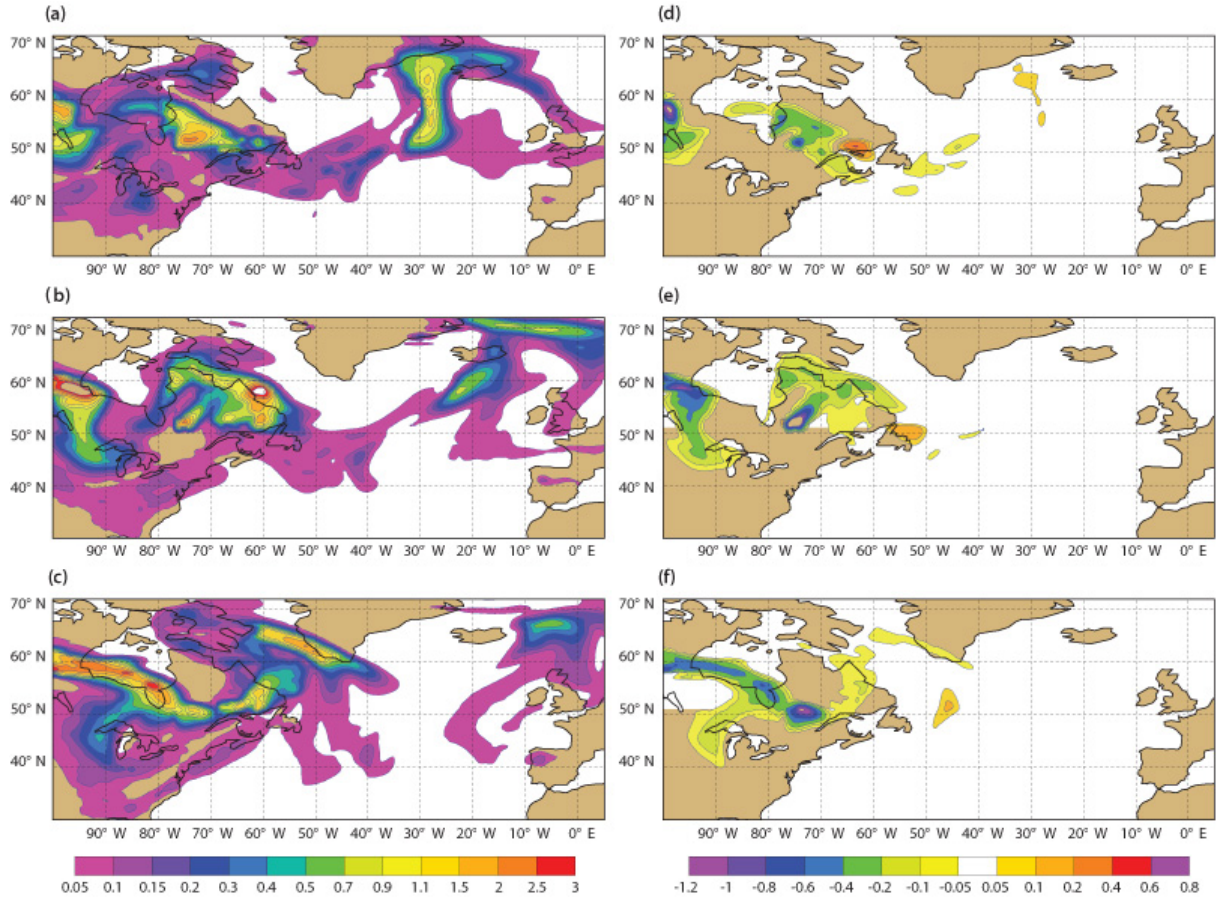

Figure 4. Panels **(a–c)** show aerosol optical depth (AOD) at 550 nm for the IFS forecast starting on 10 July 2013 and with lead times of 3 h **(a)**, 24 h **(b)** and 48 h **(c)** using the operational GFAS with the observation operator equal to persistence. Panels **(d–f)** show the difference in AOD between the two methods using the classical GFAS–persistence and the GFAS–FWI observation operator; **(d)** 3 h, **(e)** 24 h and **(f)** 48 h.

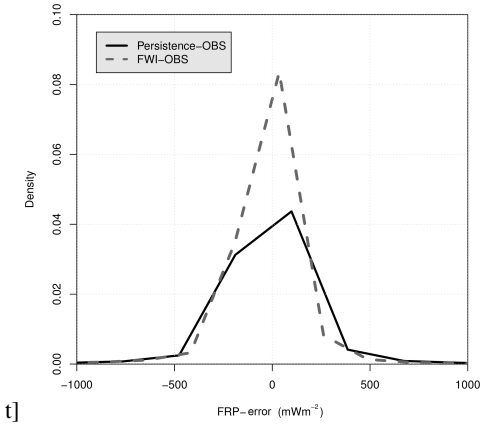

t]

Figure 5. Global verification of FRP against observations. Probability density functions (PDFs) of the observed FRP departure of MODIS compared to the two observation operator models relying on the assumption of persistence and on the FWI.

the probability density function (PDF) of the differences between the observed FRP and the two methods for the whole 3-month period. The comparison is performed using FRP of the previous day for the persistence and FRP $\cdot\, \mathcal{O}$ for the FWI experiment. Globally observed FRP values span a vast range, with a mean of 0.14 W m^{-2} and standard deviation of 0.7 W m^{-2}. If persistence is assumed from the previous day the FRP is on average 40 % (mean error: 0.21 W m^{-2}) higher than observations. This highlights the most important limitation of using persistence which never predicts a lower value for the FRP. The bias in the FRP is reduced by the introduction of the new observation operator based on the FWI (mean error 0.16 W m^{-2}). In the new approach changes in FWI are used to predict changes in FRP. The accuracy of this assumption depends on how good a predictor of fire evolution FWI is. The FWI was developed to describe fire danger and behaviour for the boreal forests of Canada and its accuracy might be lower for different vegetation. To understand the expected reduction of error in different ecosystems Fig. 6 partitions the results shown in Fig. 5 by land cover us-

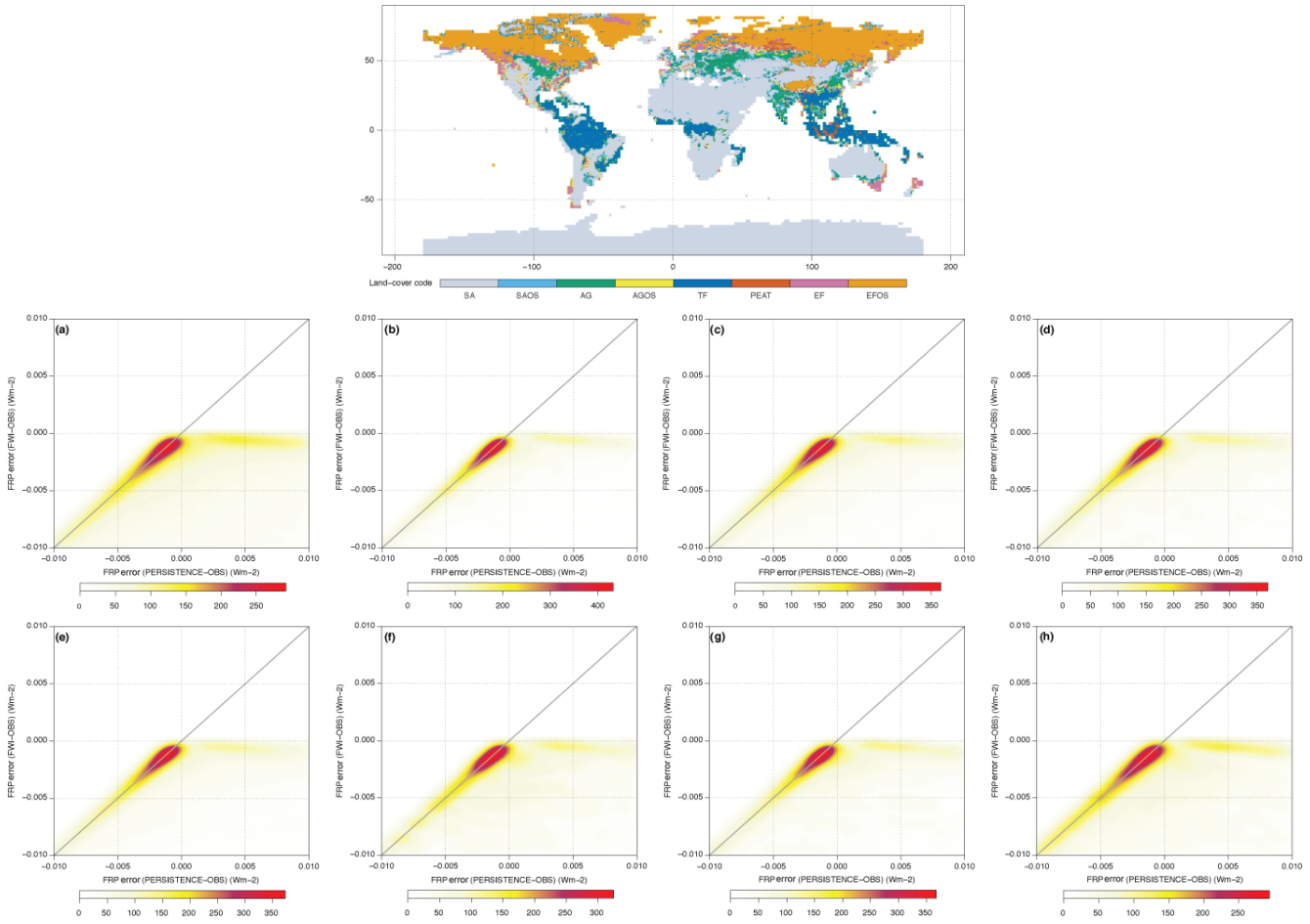

Figure 6. (a–d) Land cover class map based on dominant fire type in GFEDv3.1 and organic soil and peat maps. Gaps in land areas have been filled. See Kaiser et al. (2012) for details. **(e–h)** Two-dimensional probability density functions (PDFs) of the observed FRP departure of MODIS compared to the two observation operator models relying on the assumption of persistence and on the FWI. The PDF refers to different land covers: **(a)** savanna (SA), **(b)** savanna with organic soil (SAOS), **(c)** agriculture (AG), **(d)** agriculture with organic soil (AGOS), **(e)** tropical forest (TF), **(f)** peat (PEAT), **(g)** extratropical forest (EF), and **(h)** extratropical forest with organic soil (EFOS).

ing GFAS classification. In the GFAS the land cover classes are derived from the dominant burning land cover type in GFED3.1 and additional organic soil and peat maps (full details are given in Heil et al., 2010). The density plots show a substantial reduction of the overestimation errors for all land cover types. One interesting aspect is that positive biases are reduced more than negative ones. This behaviour can be explained noticing that the distribution of FWI, by using FWI values only when fire events are observed, is conditionally sampled towards high values (Di Giuseppe et al., 2017). At extreme values, the FWI flattens out and increases in its value are limited. Instead an increase in precipitation and humidity can produce a sudden FWI decrease, which translates into a large negative value for the modulation factor. Negative FWI increments are therefore larger than positive ones. This asymmetric behaviour means that errors are mostly corrected for overestimation of FRP in missing observation locations.

Aerosol optical depth (AOD) verification is difficult to perform in a statistically robust way as AOD observations are usually sparse in regions where fires are ignited and, as shown, changes in AOD tend to be local. However Fig. 7 shows the daily variations of aerosol optical depth (at 550 nm) observed at two stations in the proximity of Hudson Bay. Both Pickle Lake and Chapais are part of AERONET, which provides globally distributed observations of spectral AOD, inversion products and precipitable water in diverse aerosol regimes (Holben et al., 1998). Measurements are compared with CAMS forecasts over the first 24 h using fire emissions from the operational GFAS and the updated version with the FWI-based model. For these stations, the impact of our proposed modification is mainly beneficial. For example, the overestimation in AOD on 12 July 2013 is nearly halved using the new observation operator. AOD forecasts were also improved at other AERONET stations in the region, such as Waskesiu (not shown). In total there

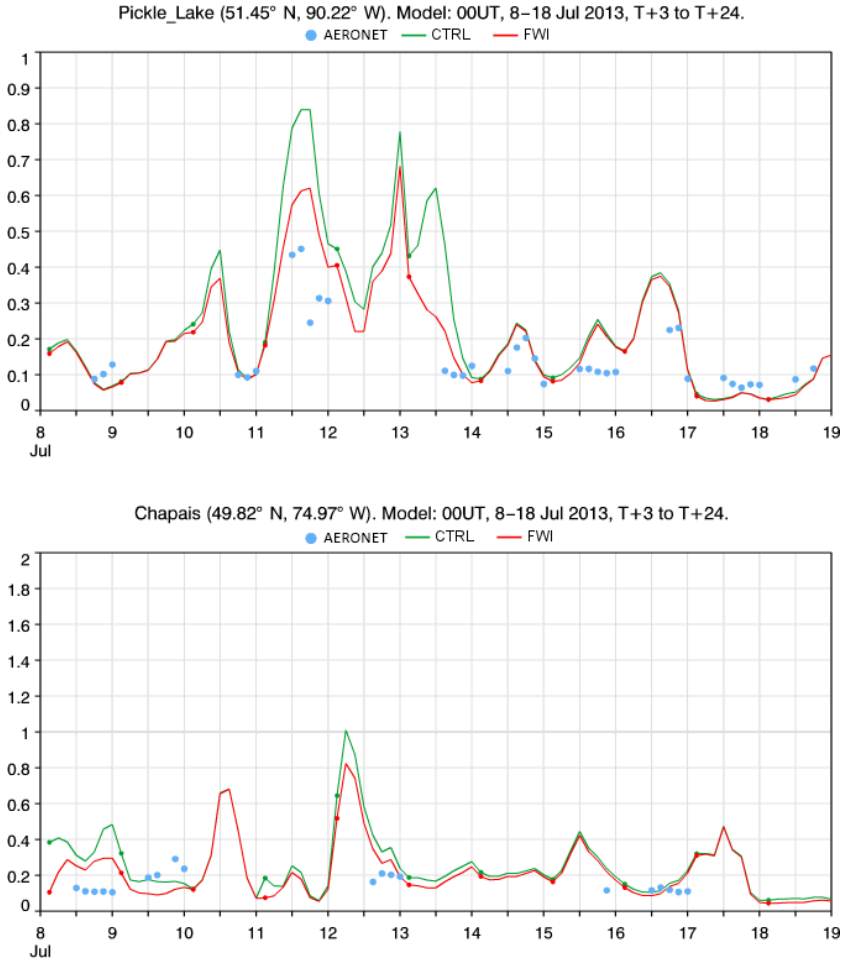

Figure 7. Local verification against observations. AOD at 550 nm evolution at two AERONET stations (Pickle Lake and Chapais), which are in the proximity of Hudson Bay. Local measurements are compared to the two models' simulations nearest grid point. The model simulations are a concatenation of 24 h forecasts. The start of the forecast is marked with a dot.

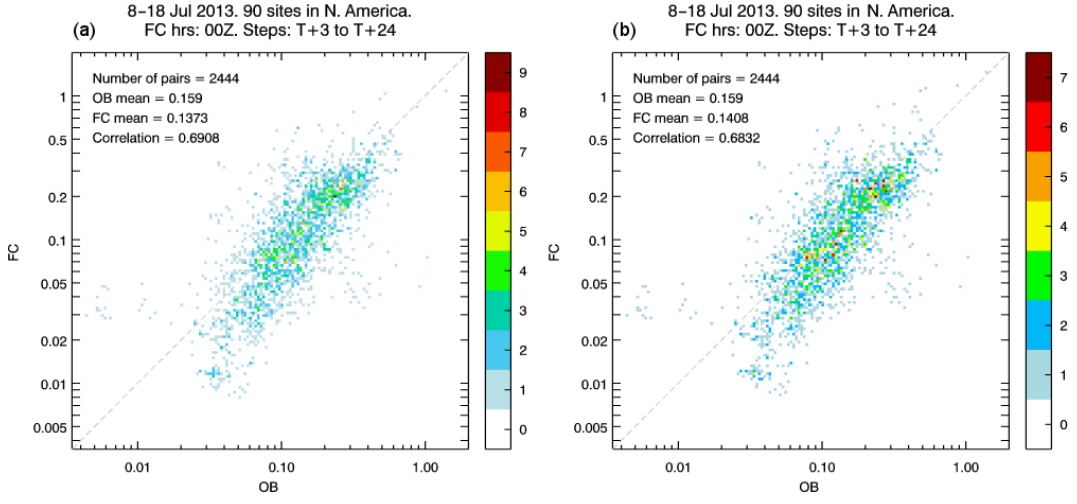

Figure 8. AOD at 550 nm for the 90 AERONET stations in North America and the two CAMS simulations initialized with the operational GFAS **(a)** and using the new FWI-based model **(b)**. The model simulations are a concatenation of the first 24 h forecasts.

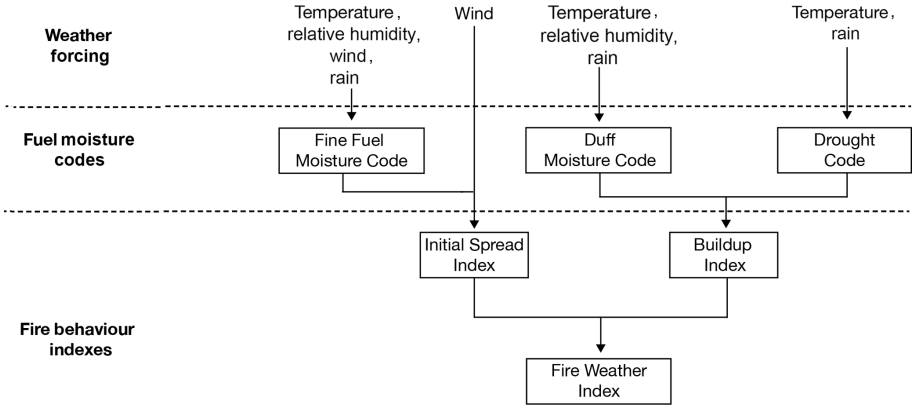

Figure 9. Schematic structure of the FWI.

were observations recorded at 90 AERONET stations covering North America for the period of interest, and looking at global statistics, there is a small benefit in adopting the FWI method in the GFAS (Fig. 8).

4 Conclusions

In this paper we have proposed a new approach to improve the estimation of fire emissions from fire radiative power (FRP) observations. The method, based on the likelihood of fire persistence evaluated using the Fire Weather Index (FWI) has been implemented in the Global Fire Assimilation System (GFAS) to substitute the simple assumption of persistence in the case where there are missing observations.

Results show that the new FWI-based observation operator is a more accurate predictor of FRP in cases where there are missing observations. In particular, the overestimation of fire duration present in the operational GFAS is substantially reduced. Moreover the new fire-related emissions also have a positive impact on the aerosol forecast of the CAMS atmospheric composition system. The impact on the AOD forecasts during a large fire event in Canada in summer 2013 is large close to the fires and negligible elsewhere. One of the advantages of the new approach is that the concept of modelling the likelihood of fire persistence as a function of weather parameters can also be extended to modulate the contribution of fire emission during the model integration. This is investigated in Di Giuseppe et al. (2017).

Data availability. All operational GFAS data are available from the ECMWF web application (http://apps.ecmwf.int/datasets/data/cams-gfas/, CAMS, 2015). The data from the modified GFAS experiments described in this paper are instead stored under experiment identification "gdpd" and "gdpe" in the operational ECMWF MARS archive. They are accessible upon request to the corresponding author or through direct download if one is a registered user of ECMWF.

Appendix A: Fire Weather Index calculation

A schematic illustration of the Fire Weather Index modelling components, their interactions and the necessary weather forcing is illustrated in Fig. 9.

The first step in the FWI calculation is the evaluation of the fuel moisture content. In the FWI biomass fuel is approximated with three non-interacting fuel layers characterized by their fast or slow response to the atmospheric forcing. The Fine Fuel Moisture Code (FFMC) provides a rating of the moisture in the litter and fine fuel occupying the first layer at the interface with the atmosphere. The Duff Moisture Code (DMC) characterizes the moisture of an intermediate layer, which consists of loosely compacted organic material, and finally the Drought Code (DC) calculates the moisture retained at the bottom where there is a deep, compact organic layer. After the diagnostic calculations of fuel moisture content in these three layers, the model calculates fire behaviour indexes in terms of rate of fire spread (Initial Spread Index, ISI) and fuel available for combustion (Buildup Index, BUI), taking into account the conditions of the previous day. Finally the FWI integrates these last-mentioned two quantities to produce a unit-less open-scale index of general fire intensity potential.

Competing interests. The authors declare that they have no conflict of interest.

Acknowledgements. This work was funded by the EU Project ANYWHERE (contract 700099) and the Global Fire Contract 389730 between the Joint Research Centre and the ECMWF. Angela Benedetti is thanked for the fruitful discussions concerning the interpretation of the MOPITT comparison. We would like to thank NASA and the MOPITT team for the ease of access to their data. Luke Jones is acknowledged for his support in creating Fig. 7. Rebecca Emerton and Sue Dunning kindly read the manuscript before submission.

Edited by: Dominick Spracklen
Reviewed by: two anonymous referees

References

Buizza, R., Milleer, M., and Palmer, T.: Stochastic representation of model uncertainties in the ECMWF ensemble prediction system, Q. J. Roy. Meteorol. Soc., 125, 2887–2908, 1999.

CAMS – the Copernicus Atmosphere Monitoring Service team: Global Fire Assimilation System v2.1, Fire Radiative Power, ECMWF, http://apps.ecmwf.int/datasets/data/cams-gfas/, 2015.

Crutzen, P. J., Heidt, L. E., Krasnec, J. P., Pollock, W. H., and Seiler, W.: Biomass burning as a source of atmospheric gases CO, H_2, N_2O, NO, CH_3Cl and COS, Nature, 282, 253–256, 1979.

Deeter, M. N., Emmons, L. K., Francis, G. L., Edwards, D. P., Gille, J. C., Warner, J. X., Khattatov, B., Ziskin, D., Lamarque, J.-F., Ho, S.-P., Yudin, V., Attié, J.-L., Packman, D., Chen, J., Mao, D., and Drummond, J. R.: Operational carbon monoxide retrieval algorithm and selected results for the MOPITT instrument, J. Geophys. Res., 108, 4399, https://doi.org/10.1029/2002JD003186, 2003.

Deeter, M. N., Martínez-Alonso, S., Edwards, D. P., Emmons, L. K., Gille, J. C., Worden, H. M., Sweeney, C., Pittman, J. V., Daube, B. C., and Wofsy, S. C.: The MOPITT Version 6 product: algorithm enhancements and validation, Atmos. Meas. Tech., 7, 3623–3632, https://doi.org/10.5194/amt-7-3623-2014, 2014.

De Groot, W. J., Landry, R., Kurz, W. A., Anderson, K. R., Englefield, P., Fraser, R. H., Hall, R. J., Raymond, D. A., Decker, V., Lynham, T. J., and Pritchard, J. M.: Estimating direct carbon emissions from Canadian wildland fires, Int. J. Wildland Fire, 16, 593–606, 2007.

Di Giuseppe, F., Pappenberger, F., Wetterhall, F., Krzeminski, B., Camia, A., Libertá, G., and San Miguel, J.: The potential predictability of fire danger provided by numerical weather prediction, J. Appl. Meteorol. Clim., 55, 2469–2491, 2016.

Di Giuseppe, F., Remy, S., Peppenberger, F., and Wetterhall, F.: Improving the forecast of biomass burning emissions with the fire weather index, J. Appl. Meteorol. Clim., 56, 2789–2799, https://doi.org/10.1175/JAMC-D-16-0405.1, 2017.

Flannigan, M. D., Logan, K. A., Amiro, B. D., Skinner, W. R., and Stocks, B.: Future area burned in Canada, Climatic Change, 72, 1–16, 2005.

Flannigan, M. D., Krawchuk, M. A., de Groot, W. J., Wotton, B. M., and Gowman, L. M.: Implications of changing climate for global wildland fire, Int. J. Wildland Fire, 18, 483–507, 2009.

Flemming, J., Huijnen, V., Arteta, J., Bechtold, P., Beljaars, A., Blechschmidt, A.-M., Diamantakis, M., Engelen, R. J., Gaudel, A., Inness, A., Jones, L., Josse, B., Katragkou, E., Marecal, V., Peuch, V.-H., Richter, A., Schultz, M. G., Stein, O., and Tsikerdekis, A.: Tropospheric chemistry in the Integrated Forecasting System of ECMWF, Geosci. Model Dev., 8, 975–1003, https://doi.org/10.5194/gmd-8-975-2015, 2015.

French, N. H. F., Goovaerts, P., and Kasischke, E. S.: Uncertainty in estimating carbon emissions from boreal forest fires, J. Geophys. Res.-Atmos., 109, D14S08, https://doi.org/10.1029/2003JD003635, 2004.

Heil, A., Kaiser, J. W., van der Werf, G. R., Wooster, M. J., Schultz, M. G., and van der Gon, H. D.: Assessment of the real-time fire emissions (GFASv0) by MACC, Tech. Memo 628, European Centre for Medium-Range Weather Forecasts, Reading, UK, 2010.

Holben, B., Eck, T., Slutsker, I., Tanre, D., Buis, J., Setzer, A., Vermote, E., Reagan, J., Kaufman, Y., Nakajima, T., Lavenu, F., Jankowiak, I., and Smirnov, A.: AERONET – A federated instrument network and data archive for aerosol characterization, Remote Sens. Environ., 66, 1–16, 1998.

Kaiser, J. W., Heil, A., Andreae, M. O., Benedetti, A., Chubarova, N., Jones, L., Morcrette, J.-J., Razinger, M., Schultz, M. G., Suttie, M., and van der Werf, G. R.: Biomass burning emissions estimated with a global fire assimilation system based on observed fire radiative power, Biogeosciences, 9, 527–554, https://doi.org/10.5194/bg-9-527-2012, 2012.

Kalnay, E.: Atmospheric modeling, data assimilation, and predictability, Cambridge University Press, Cambridge, 2003.

Karl, T., Guenther, A., Yokelson, R. J., Greenberg, J., Potosnak, M., Blake, D. R., and Artaxo, P.: The tropical forest and fire emissions experiment: Emission, chemistry, and transport of biogenic volatile organic compounds in the lower atmosphere over Amazonia, J. Geophys. Res.-Atmos., 112, D18302, https://doi.org/10.1029/2007JD008539, 2007.

Kasischke, E. S. and Bruhwiler, L. P.: Emissions of carbon dioxide, carbon monoxide, and methane from boreal forest fires in 1998, J. Geophys. Res.-Atmos., 107, 8146, https://doi.org/10.1029/2001JD000461, 2002.

Kaufman, Y., Ichoku, C., Giglio, L., Korontzi, S., Chu, D., Hao, W., Li, R.-R., and Justice, C.: Fire and smoke observed from the Earth Observing System MODIS instrument – products, validation, and operational use, Int. J. Remote Sens., 24, 1765–1781, 2003.

Lee, B., Alexander, M., Hawkes, B., Lynham, T., Stocks, B., and Englefield, P.: Information systems in support of wildland fire management decision making in Canada, Comput. Elect. Agricult., 37, 185–198, 2002.

Roberts, G., Wooster, M., Freeborn, P., and Xu, W.: Integration of geostationary FRP and polar-orbiter burned area datasets for an enhanced biomass burning inventory, Remote Sens. Environ., 115, 2047–2061, 2011.

Stocks, B. J., Lynham, T., Lawson, B., Alexander, M., Van Wagner, C., McAlpine, R., and Dube, D.: Canadian forest fire danger rating system: an overview, Forestry Chronicle, 65, 258–265, 1989.

van der Werf, G. R., Randerson, J. T., Giglio, L., Collatz, G. J., Kasibhatla, P. S., and Arellano Jr., A. F.: Interannual variability in global biomass burning emissions from 1997 to 2004, Atmos. Chem. Phys., 6, 3423–3441, https://doi.org/10.5194/acp-6-3423-2006, 2006.

Van Wagner, C.: Equations and FORTRAN program for the Canadian Forest Fire Weather Index System, Forestry Technical Report 33, Canadian Forestry Service, Petawawa National Forestry Institute, Chalk River, Ontario, p. 18, 1985.

Van Wagner, C.: Development and Structure of the Canadian Forest Fire Weather Index System, Technical Report 35, Citeseer, Canadian Forestry Service, Headquarters, Ottawa, p. 35, 1987.

Wooster, M. J., Roberts, G., Perry, G., and Kaufman, Y.: Retrieval of biomass combustion rates and totals from fire radiative power observations: FRP derivation and calibration relationships between biomass consumption and fire radiative energy release, J. Geophys. Res.-Atmos., 110, D24311, https://doi.org/10.1029/2005JD006318, 2005.

Yokelson, R. J., Christian, T. J., Karl, T. G., and Guenther, A.: The tropical forest and fire emissions experiment: laboratory fire measurements and synthesis of campaign data, Atmos. Chem. Phys., 8, 3509–3527, https://doi.org/10.5194/acp-8-3509-2008, 2008.